
Taming Tail Risk in Financial Markets: Conformal Risk Control for Nonstationary Portfolio VaR

Marc Schmitt¹

Abstract

Risk forecasts drive trading constraints and capital allocation, yet losses are nonstationary and regime-dependent. This paper studies sequential one-sided VaR control via conformal calibration. I propose regime-weighted conformal risk control (RWC), which calibrates a safety buffer from past forecast errors using exponential time decay and regime-similarity weights from regime features. RWC is model-agnostic and wraps any conditional quantile forecaster to target a desired exceedance rate. Finite-sample coverage is established under weighted exchangeability, and approximation bounds are derived under smoothly drifting regimes. On the CRSP U.S. equity portfolio, time-weighted conformal calibration is a strong default under drift, while regime weighting can improve regime-conditional stability in some settings with modest conservativeness changes.

1. Introduction

Forecasting and controlling tail risk in financial markets is notoriously difficult. Return distributions are heavy-tailed, exhibit volatility clustering, and shift over time; even if the conditional distribution is well-modeled within a regime, it can drift rapidly during crises or structural change. Moreover, this nonstationarity is often regime-structured: volatility and tail behavior cluster into persistent states (e.g., calm vs stress), as in regime-switching models (Hamilton, 1989; Gray, 1996; Engle & Rangel, 2008). As a result, value-at-risk (VaR) forecasts can be miscalibrated, with realized VaR exceedance rates deviating substantially from nominal targets, especially in stress periods (Berkowitz & O’Brien, 2002). These calibration failures matter because VaR-type constraints directly affect leverage and risk-taking (Basak & Shapiro, 2001; Adrian & Shin, 2014).

Conformal prediction is appealing for risk control because it can wrap black-box forecasters and provide finite-sample guarantees under exchangeability. However, financial data are sequential and nonstationary, so classical conformal validity can fail under time dependence and distribution shift. Prior work addresses covariate shift via importance weighting (Tibshirani et al., 2019), sequential nonstationarity via adaptive updates (Gibbs & Candès, 2021), and dynamics in time series (Xu & Xie, 2021). In finance, drift is pervasive and often regime-structured, so calibration should remain stable within regimes. This work is complementary to Conformal Risk Control (Angelopoulos et al., 2024), which controls the expected value of a monotone loss functional. In contrast, sequential one-sided quantile risk (VaR exceedances) is targeted in nonstationary, regime-structured time series and calibration is adapted by recency and regime-similarity weighting of conformity scores.

Recency weighting alone often stabilizes calibration under drift: the resulting time-weighted conformal calibration (TWC) is a strong, computationally simple default. Building on this, RWC adds regime-similarity weighting to target regime-conditional calibration when market conditions recur (e.g., volatility regimes), at the cost of reducing the effective calibration sample size. This leads to a natural empirical question: when does regime weighting improve stability beyond time weighting, and what is the conservativeness tradeoff?

Contributions.

- Sequential VaR control under nonstationarity is formalized and metrics for regime-conditional calibration are proposed.
- RWC is introduced, combining recency and regime-similarity weighting to adapt conformal calibration to drift.
- Finite-sample guarantees under weighted exchangeability are proved and error is bounded under smoothly drifting regime-conditional distributions.
- TWC is a strong default, while regime weighting can improve regime-conditional stability with modest additional conservativeness.

¹University of Oxford. Correspondence to: Marc Schmitt <marc.schmitt [at] cs.ox.ac.uk>.

2. Background and related work

Conformal prediction provides finite-sample marginal coverage guarantees under exchangeability (Vovk et al., 2005; Shafer & Vovk, 2008). For regression, conformalized quantile regression (CQR) yields adaptive, heteroscedastic intervals by conformalizing estimated conditional quantiles (Romano et al., 2019). This provides a direct template for conformalizing quantile forecasts; a one-sided VaR bound can be viewed as a sequential, tail-focused analogue in which an additive safety buffer is calibrated on a $(1 - \alpha)$ quantile forecaster. Weighted conformal methods extend this framework to certain forms of distribution shift by computing weighted quantiles of past conformity scores, often using density-ratio weights (Tibshirani et al., 2019). The same weighted conformal mechanism is adopted, but weights are derived from recency and regime similarity rather than density ratios, which underpins the weighted-exchangeability guarantee.

Recent work generalizes conformal prediction from coverage guarantees to risk control. Conformal Risk Control (CRC) controls the expectation of a monotone loss functional and discusses variants under distribution shift (Angelopoulos et al., 2024; Snell & Griffiths, 2025). This setting differs in both objective and structure: sequential control of VaR exceedances in nonstationary financial time series is targeted, specialization is to one-sided quantile bounds, and adaptation is achieved by localizing the calibration score distribution toward relevant historical observations.

Nonstationarity has been explicitly addressed in sequential and time-series conformal inference. Adaptive conformal inference (ACI) dynamically adjusts the effective miscoverage level to maintain calibration under drift (Gibbs & Candès, 2021), and ACI is used as a primary baseline. In contrast, the target exceedance level is kept fixed and adaptation is achieved by reweighting the calibration scores. For time series, EnbPI provides bootstrap-based conformal intervals for dynamic sequences (Xu & Xie, 2021), with subsequent work developing sequential predictive conformal inference (Xu & Xie, 2023). Related approaches cast sequential conformal calibration as a control problem, using feedback mechanisms to track recent miscoverage (Angelopoulos et al., 2023); this approach instead emphasizes relevance-based localization via time decay and regime similarity.

A growing theoretical literature studies conformal guarantees beyond exchangeability. General validity results justify asymmetric and weighted conformal constructions in drifting or non-i.i.d. settings (Barber et al., 2023), providing a principled foundation for recency- and regime-weighted calibration. Online analyses further characterize conformal inference under arbitrary sequential distribution shifts (Gibbs & Candès, 2024), offering a complementary perspective on nonstationary deployment.

Exact distribution-free conditional coverage is fundamentally impossible in general (Barber et al., 2021), motivating practical forms of localized or group-conditional calibration. Localized conformal prediction adapts score distributions to neighborhoods in feature space (Guan, 2023), while class-conditional conformal methods provide stratified coverage across groups (Ding et al., 2023). Regime-weighted calibration can be viewed as a continuous analogue of such stratification, designed to stabilize exceedance rates across recurring market regimes.

Finally, VaR is a quantile-based tail risk measure widely used in practice, while CVaR (expected shortfall) captures tail severity (Rockafellar & Uryasev, 2000; Engle & Manganelli, 2004). Empirical studies document systematic VaR model failures, particularly during stress periods (Berkowitz & O'Brien, 2002), motivating calibration layers that remain reliable under nonstationarity. Standard VaR backtests evaluate unconditional exceedance rates and independence (Kupiec, 1995; Christoffersen, 1998). This focus is complementary: predictive VaR bounds targeting a desired exceedance level are constructed and stability across regimes is emphasized.

3. Problem setup: sequential portfolio risk control

A time series of covariates and portfolio losses is observed:

$$(x_t, y_t) \in \mathcal{X} \times \mathcal{Y}, \quad t = 1, 2, \dots, T,$$

where x_t summarizes information available at time t (e.g., recent returns, realized volatility), and y_t is the realized next-period portfolio loss (e.g., $y_t = -r_t^{\text{port}}$ for one-day return r_t^{port}). Let $\alpha \in (0, 1)$ denote a target miscoverage level (e.g., $\alpha = 0.01$ for 99% VaR control). A one-sided VaR bound at level $1 - \alpha$ is a function $U_t(x_t)$ such that

$$\mathbb{P}(y_t \leq U_t(x_t)) \geq 1 - \alpha. \quad (1)$$

In nonstationary settings, the distribution of (x_t, y_t) may vary with t . Procedures are therefore studied that aim to keep empirical exceedance rates close to α over time and within market regimes.

Timing convention (causality). Throughout, x_t denotes the information set available *strictly before* the loss y_t is realized. For daily close-to-close data, y_t is the loss over trading day t (i.e., from day $t-1$ close to day t close), so $y_t = -r_t^{\text{port}}$ with r_t^{port} the $t-1 \rightarrow t$ return. All components of x_t (and regime features $z_t = g(x_t)$) are computed using data available up through day $t-1$. Thus the procedure observes x_t , outputs $U_t(x_t)$, and only then observes y_t , matching Algorithm 1.

Base quantile forecaster. Let $\hat{q}_t = f_t(x_t)$ denote a prediction of the conditional $(1 - \alpha)$ -quantile of y_t produced by an arbitrary forecaster f_t trained on past data (e.g., rolling-window quantile regression, GARCH-based VaR). Conformal risk control constructs an adjusted bound

$$U_t = \hat{q}_t + \hat{c}_t,$$

where \hat{c}_t is a data-driven safety buffer calibrated from past forecast errors.

Conformity scores. The one-sided conformity score at time t is defined as

$$s_t := y_t - \hat{q}_t, \quad (2)$$

so that large positive s_t indicates the base model underpredicted tail risk. A conformal adjustment \hat{c}_t is typically a high quantile of past scores $\{s_i\}$.

4. Method: Regime-weighted conformal calibration

RWC is introduced, which calibrates \hat{c}_t using a weighted quantile of past conformity scores. The weights emphasize (i) recency, to adapt under drift, and (ii) regime similarity, to improve regime-conditional stability when conditions recur.

4.1. Regime representation and weighting

Let $z_t = g(x_t) \in \mathbb{R}^d$ be a *regime embedding* computed from covariates, intended to capture market conditions such as volatility level and trend. In experiments, interpretable regime features are used, but g can be any fixed mapping.

For a current time t and a calibration index $i < t$, assign weight

$$w_i(t) \propto \underbrace{\exp(-\lambda(t-i))}_{\text{recency}} \cdot \underbrace{K_h(z_i, z_t)}_{\text{regime similarity}}, \quad (3)$$

where $\lambda \geq 0$ is a decay rate and K_h is a positive kernel (e.g., Gaussian) with bandwidth h :

$$K_h(z_i, z_t) = \exp\left(-\frac{1}{2h^2} \|z_i - z_t\|^2\right).$$

Thus recent scores and scores from similar regimes receive higher weight.

Preprocessing of regime features. Because K_h depends on Euclidean distances, each coordinate of z_t is standardized to zero mean and unit variance using training-period statistics (to avoid test leakage), and the same transform is applied at validation and test time. Bandwidths h are reported in standardized units.

Weighted conformal inference. Importance-weighted conformal calibration corrects covariate shift by weighting scores via density ratios (Tibshirani et al., 2019). More broadly, conformal validity can extend beyond exchangeability via carefully designed asymmetric weighting schemes (Barber et al., 2023). In RWC, time decay prioritizes recent history under drift, while kernel similarity localizes calibration to comparable market regimes.

4.2. Weighted conformal quantile

Calibration index set. Let m be the maximum calibration-buffer size. At time t , let $\mathcal{I}_t \subset \{1, \dots, t-1\}$ denote the available score indices just before issuing the time- t bound. The recent window used is

$$\mathcal{I}_t := \{i : \max\{1, t-m\} \leq i \leq t-1\}.$$

When $t-1 < m$, this reduces to $\mathcal{I}_t = \{1, \dots, t-1\}$. Conformalized bounds are issued once \mathcal{I}_t is nonempty; denote the first such time by t_0 .

Weighted quantile threshold. Given scores $\{s_i\}_{i \in \mathcal{I}_t}$ and unnormalized weights $\{w_i(t)\}_{i \in \mathcal{I}_t}$ from (3), define normalized weights $\tilde{w}_i(t) := w_i(t) / \sum_{j \in \mathcal{I}_t} w_j(t)$. RWC sets

$$\hat{c}_t := Q_{1-\alpha}^{\tilde{w}(t)}(\{s_i\}_{i \in \mathcal{I}_t}), \quad (4)$$

the weighted $(1-\alpha)$ -quantile of the score distribution (using the standard “smallest c such that cumulative weight $\geq 1-\alpha$ ” definition; see Section A). Finally, output $U_t = \hat{q}_t + \hat{c}_t$.

Finite-sample correction (optional). For exact finite-sample validity as in Theorem 5.2, one can replace the level $1 - \alpha$ in (4) by the inflated level ρ_t in (5). In experiments, $1 - \alpha$ is used; when the total calibration weight W_t (or $n_{\text{eff}}(t)$) is large, the difference is typically negligible.

4.3. Baselines

RWC is compared to three sequential conformal calibrators: (i) SWC: sliding-window conformal with an unweighted window of the last m scores; (ii) TWC: time-weighted conformal using only recency weights (set $K_h \equiv 1$); (iii) ACI (Gibbs & Candès, 2021): adaptive conformal inference that updates an effective miscoverage level to track drift.

5. Theory

Classical conformal guarantees rely on exchangeability, which is typically violated by dependent and drifting financial time series. Still, exact finite-sample results under idealized symmetry assumptions are useful as a benchmark: they clarify how weighting yields validity and connect RWC to weighted conformal prediction (Tibshirani et al.,

Algorithm 1 RWC: Regime-Weighted Conformal VaR

```

1: Input: target  $\alpha$ ; base forecaster  $f_t$ ; calibration size  $m$ ;
   decay  $\lambda$ ; kernel  $K_h$ ; regime map  $g$ ; ESS threshold  $n_{\min}$ 
2: Initialize empty buffers for past scores  $\{s_i\}$  and embed-
   dings  $\{z_i\}$ 
3: for  $t = t_0, t_0+1, \dots, T$  do
4:   Observe covariates  $x_t$  (available before  $y_t$ ) and com-
      pute  $z_t = g(x_t)$ 
5:   Train/update base model  $f_t$  on past data; predict  $\hat{q}_t =$ 
       $f_t(x_t)$ 
6:   Form weights  $w_i(t) \propto \exp(-\lambda(t-i)) \cdot K_h(z_i, z_t)$ 
      for  $i \in \mathcal{I}_t$ 
7:   Normalize  $\tilde{w}_i(t) \leftarrow w_i(t) / \sum_{j \in \mathcal{I}_t} w_j(t)$ 
8:   Compute  $n_{\text{eff}}(t) \leftarrow 1 / \sum_{i \in \mathcal{I}_t} \tilde{w}_i(t)^2$ 
9:   if  $n_{\text{eff}}(t) < n_{\min}$  then
10:    Set  $K_h \equiv 1$  for this step (fallback to time-only
      weights) and recompute  $\tilde{w}_i(t) \propto \exp(-\lambda(t-i))$ 
11:   end if
12:   Compute  $\hat{c}_t \leftarrow Q_{1-\alpha}^{\tilde{w}(t)}(\{s_i\}_{i \in \mathcal{I}_t})$ 
13:   Output VaR bound  $U_t = \hat{q}_t + \hat{c}_t$ 
14:   Observe loss  $y_t$  and compute score  $s_t = y_t - \hat{q}_t$ 
15:   Append  $(s_t, z_t)$  to buffers; keep only most recent  $m$ 
      entries
16: end for

```

2019) and conformal validity beyond exchangeability (Barber et al., 2023). Two results are therefore presented: (1) an exact finite-sample statement under weighted exchangeability; and (2) an approximate regime-conditional bound under smooth drift, making explicit the localization–variance tradeoff induced by kernel weights. Proofs are in the appendix.

5.1. Exact coverage under weighted exchangeability

Notation. Fix time t and calibration index set $\mathcal{I}_t \subset \{1, \dots, t-1\}$. Let $w_i(t) \geq 0$ be the (unnormalized) weights in (3) for $i \in \mathcal{I}_t$, and define

$$W_t := \sum_{i \in \mathcal{I}_t} w_i(t), \quad \bar{w}_i(t) := \frac{w_i(t)}{W_t}.$$

Let $w_t(t)$ denote the test-time weight for the current point; for (3), $w_t(t) = 1$. For a finite-sample correction analogous to the usual $(m+1)$ conformal adjustment, use the inflated level

$$\rho_t := \min \left\{ 1, (1-\alpha) \left(1 + \frac{w_t(t)}{W_t} \right) \right\}. \quad (5)$$

Define the weighted threshold

$$\hat{c}_t := Q_{\rho_t}^{\bar{w}(t)}(\{s_i\}_{i \in \mathcal{I}_t}), \quad (6)$$

and output $U_t = \hat{q}_t + \hat{c}_t$.

Assumption 5.1 (Weighted exchangeability). Fix time t . Conditional on (x_t, z_t) , the collection $\{(s_i, w_i(t))\}_{i \in \mathcal{I}_t} \cup \{(s_t, w_t(t))\}$ is weighted exchangeable in the sense of Tibshirani et al. (2019).

Theorem 5.2 (Finite-sample weighted coverage). *Under Assumption 5.1, the RWC bound $U_t = \hat{q}_t + \hat{c}_t$ with \hat{c}_t defined in (6) satisfies*

$$\mathbb{P}(y_t \leq U_t \mid x_t, z_t) \geq 1 - \alpha.$$

Remark (relation to the implementation). If one uses $\rho_t = 1 - \alpha$ instead of (5), the difference is typically negligible when W_t (or the effective sample size) is large, but Theorem 5.2 uses the standard finite-sample correction.

5.2. Regime-conditional coverage under drift

Exact exchangeability is unrealistic for finance. The approximation error is therefore analyzed when score distributions vary smoothly across regimes and drift gradually over time, so that emphasizing recent and regime-similar calibration points yields near-valid coverage.

Assumption 5.3 (Smooth regime drift and gradual time variation). Let $F_t(u \mid z)$ denote the conditional CDF of the score s_t given $z_t = z$. There exist constants $L_z, L_t > 0$ such that for all $z, z' \in \mathbb{R}^d$ and all $u \in \mathbb{R}$,

$$|F_t(u \mid z) - F_t(u \mid z')| \leq L_z \|z - z'\|.$$

Moreover, for all $i < t$ and all $u \in \mathbb{R}$,

$$|F_t(u \mid z_t) - F_t(u \mid z_i)| \leq L_t |t - i|.$$

Finally, $\{z_t\}$ is bounded and the kernel K_h is Lipschitz and concentrates its mass within $\|z_i - z_t\| = O(h)$ under the normalized weights.

Effective weighted sample size. Let $\bar{w}_i(t)$ denote the normalized calibration weights and define

$$n_{\text{eff}}(t) := \frac{1}{\sum_{i \in \mathcal{I}_t} \bar{w}_i(t)^2}. \quad (7)$$

Theorem 5.4 (Approximate regime-conditional coverage under smooth drift (informal)). *Under Assumption 5.3 and mild regularity of the weighted quantile estimator, RWC achieves*

$$\mathbb{P}(y_t \leq U_t \mid z_t) \geq 1 - \alpha - \varepsilon_t,$$

where the coverage gap admits a decomposition

$$\varepsilon_t = O(L_z h) + O(L_t \tau_t) + O\left(\sqrt{\frac{1}{n_{\text{eff}}(t)}}\right),$$

with $\tau_t := \sum_{i \in \mathcal{I}_t} \bar{w}_i(t) (t - i)$ the effective lag under the normalized weights (for TWC this depends only on recency);

for RWC it reflects both recency and regime similarity). The stochastic term corresponds to concentration of the weighted empirical CDF and holds under independence and, more generally, under sufficiently weak dependence (e.g., mixing conditions) up to log factors.

Discussion. Theorem 5.4 motivates choosing h small enough to localize to similar regimes while maintaining a sufficiently large $n_{\text{eff}}(t)$. The recency parameter λ controls the effective memory, trading off faster adaptation against increased variance. In practice, (λ, h, m) are tuned on a validation period to balance calibration, regime stability, and conservativeness.

6. Experiments

6.1. Data and portfolio

Data. Daily U.S. equity data from the CRSP value-weighted market index (accessed via WRDS) are used, spanning 1990-03-30 through 2024-12-31 (8755 trading days). CRSP is the benchmark dataset in empirical asset pricing and risk management, providing survivorship-bias-free coverage, accurate return adjustments for dividends and other corporate actions, and a long, internally consistent historical record spanning multiple business cycles and crisis regimes. These properties make CRSP particularly well suited for evaluating tail-risk control and calibration stability under nonstationarity. The daily loss is defined as

$$y_t = -r_t^{\text{port}},$$

where r_t^{port} denotes the portfolio return at time t .

Sample period and splits. A chronological split is adopted: training (1990-03-30–2011-01-31), validation (2011-02-01–2018-01-16), and test (2018-01-17–2024-12-31). The test period contains $N = 1751$ observations. Unless otherwise stated, all tables report test-period results (e.g., Table 5). Rolling exceedance plots show the full sample, with the test start marked by a vertical dotted line.

Regimes. Market regimes are represented using interpretable features from lagged returns and evaluation is stratified by realized-volatility quintiles. Concretely, the regime embedding z_t is built from 21-day realized volatility and 5-day mean absolute returns (definitions and preprocessing in Appendix A).

Hyperparameter tuning. Conformal hyperparameters are tuned on the validation period via grid search. For each candidate setting the validation exceedance rate $\widehat{\text{Exc}}_{\text{val}}$ and the maximum 1-year rolling exceedance $\text{RollMax}_{\text{val}}$ (252 trading days) are computed, and hyperparameters are selected by minimizing $|\widehat{\text{Exc}}_{\text{val}} - \alpha| +$

$0.5 \max\{0, \widehat{\text{RollMax}}_{\text{val}} - \alpha\}$. For SWC/TWC/RWC grids $m \in \{252, 504, 756\}$, $\lambda \in \{0.002, 0.005, 0.01\}$, and $h \in \{0.5, 1, 2\}$ (RWC only) are used. For ACI, $m = 252$ is set and $\gamma \in \{0.002, 0.005, 0.01, 0.02\}$ is tuned using the same objective. Selected hyperparameters are reported in Table 7. For RWC an ESS safeguard is also applied: if $n_{\text{eff}}(t) < n_{\text{min}}$, a fallback to time-only (TWC) weights is used for that step ($n_{\text{min}} = 100$ for the GBDT base and $n_{\text{min}} = 30$ for the HS base).

6.2. Models and calibrators

Base forecasters. Two representative base VaR forecasters are considered: (i) *historical simulation* (HS), a rolling empirical $(1 - \alpha)$ quantile of past losses; and (ii) *gradient boosting quantile regression* (GBDT), fit on a rolling window of covariates. Each forecaster outputs \hat{q}_t , an estimate of the $(1 - \alpha)$ -quantile of y_t .

Conformal wrappers. SWC, TWC, ACI (Gibbs & Candès, 2021), and RWC are applied to each base model.

6.3. Metrics

The following are reported: (i) overall exceedance rate $\frac{1}{T} \sum_t \mathbf{1}\{y_t > U_t\}$; (ii) exceedance rate by regime (realized-volatility quintiles); (iii) average bound tightness $\frac{1}{T} \sum_t U_t$ (lower is tighter, subject to calibration); (iv) rolling 1-year exceedance rates; and (v) standard VaR backtests on exceedance indicators: Kupiec UC and Christoffersen IND/CC (Kupiec, 1995; Christoffersen, 1998).

6.4. Results

Out-of-sample 99% VaR control ($\alpha = 0.01$) is reported on the CRSP value-weighted market index. Table 1 summarizes overall calibration and tightness, Table 2 reports regime-stratified exceedances, and Figure 1 visualizes rolling one-year exceedance rates over time (GBDT base; the HS analogue is in Figure 2).

Calibration and tightness (Table 1). With the GBDT base (Panel A), the uncalibrated forecaster severely undercovers (5.31% exceedance at a 1% target). All wrappers bring exceedances close to target: SWC (1.37%), ACI (1.14%), TWC (1.09%), and RWC (1.14%). Differences are mainly in tightness: ACI is looser (Avg. VaR 200 bps) than weighted-quantile methods, while RWC matches ACI's exceedance with a tighter average bound (155 bps). TWC is closest to target on average (1.09%) with Avg. VaR 165 bps. With the HS base (Panel B), the uncalibrated model also undercovers (1.71%). Here regime weighting changes both calibration and tightness: RWC reduces exceedance to 1.09% while tightening the average bound (247 bps), compared to TWC (1.48%, 339 bps), SWC (1.60%, 358 bps),

Table 1. Test-set exceedance results for 99% VaR ($\alpha = 0.01$) on the CRSP value-weighted index. Panel A uses a gradient boosting quantile base forecaster; Panel B uses historical simulation.

Panel A: Gradient boosting base (GBDT)		
Method	Exceedance (%)	Avg. VaR (bps)
Base quantile model	5.31	146
SWC (rolling)	1.37	182
ACI	1.14	200
TWC (time decay)	1.09	165
RWC (time + regime)	1.14	155
Panel B: Historical simulation base (HS)		
Method	Exceedance (%)	Avg. VaR (bps)
Base quantile model	1.71	317
SWC (rolling)	1.60	358
ACI	1.26	426
TWC (time decay)	1.48	339
RWC (time + regime)	1.09	247

and ACI (1.26%, 426 bps), suggesting regime localization can matter when the base model is less adaptive.

Calibration stability over time (Figure 1). Average exceedance can mask transient miscalibration, which is particularly relevant for risk management. Rolling one-year exceedance rates therefore provide a stability diagnostic. Across the full sample, all methods vary over time (consistent with regime shifts), but conformal wrappers keep rolling exceedances much closer to the 1% target than an uncalibrated forecaster would. Methods emphasizing recency or feedback (TWC, ACI) tend to adapt more quickly, while stronger localization (RWC) can yield tighter bounds but may exhibit larger fluctuations when weights concentrate on a small subset of past observations. At $\alpha = 1\%$, rolling 252-day exceedance rates are inherently noisy—each additional exceedance shifts the curve by $1/252 \approx 0.4\%$ —so spikes are interpreted mainly as a stability signal.

Regime-conditional exceedance (Table 2). With the GBDT base (Panel A), exceedances rise with realized volatility for all methods, and the top-volatility quintile remains above the 1% target even after calibration. ACI is lowest in the top quintile (1.71%), while SWC/TWC/RWC are at 2.29%. In low-volatility regimes, methods tend to be conservative; for example in quintile 0, SWC/TWC are at 0.28% and ACI at 0.57%, while RWC is closer to target at 1.14% but slightly overshoots. Overall, with a flexible base forecaster, recency weighting and feedback-style adaptation appear to dominate incremental gains from regime similarity in stress. With the HS base (Panel B), regime weighting shows its clearest benefit in stress: in the top volatility quintile, RWC reduces exceedance to 2.86% versus 3.14% (ACI) and 3.71% (SWC/TWC). This is consistent with bias-variance tradeoffs: when the base model adapts

Table 2. Test-set exceedance rate (%) by realized-volatility quintile (Panel A: GBDT base; Panel B: HS base).

Panel A: Gradient boosting base (GBDT)					
Vol quintile	n	SWC	ACI	TWC	RWC
0	351	0.28	0.57	0.28	1.14
1	350	1.43	1.43	0.57	0.29
2	350	1.14	0.86	0.86	0.86
3	350	1.71	1.14	1.43	1.14
4	350	2.29	1.71	2.29	2.29
Panel B: Historical simulation base (HS)					
Vol quintile	n	SWC	ACI	TWC	RWC
0	351	0.00	0.00	0.00	0.00
1	350	0.57	0.57	0.57	0.57
2	350	1.43	0.86	1.43	0.86
3	350	2.29	1.71	1.71	1.14
4	350	3.71	3.14	3.71	2.86

Table 3. Regime-stability summary derived from volatility-quintile exceedances (Table 2). Metrics are in percentage points (pp) relative to the target exceedance level $\alpha = 0.01$ (1%).

Panel A: GBDT base			
Method	Reg-MAE (pp)	Reg-MaxDev (pp)	Reg-Std (pp)
SWC	0.66	1.29	0.66
ACI	0.37	0.71	0.40
TWC	0.60	1.29	0.71
RWC	0.49	1.29	0.65
Panel B: HS base			
Method	Reg-MAE (pp)	Reg-MaxDev (pp)	Reg-Std (pp)
SWC	1.17	2.71	1.31
ACI	0.89	2.14	1.09
TWC	1.06	2.71	1.27
RWC	0.71	1.86	0.96

slowly, emphasizing regime-similar history can reduce systematic undercoverage in high-volatility states.

When does regime weighting help? The mixed behavior across base forecasters aligns with the localization-variance tradeoff in Theorem 5.4. Regime weighting can reduce bias by emphasizing regimes closer to the current z_t (the $O(L_z h)$ term), but can increase variance by reducing the effective sample size $n_{\text{eff}}(t)$ (the $O(\sqrt{1/n_{\text{eff}}(t)})$ term). When the base model is already flexible (GBDT), time decay alone often tracks much of the drift, so additional localization may mostly reduce $n_{\text{eff}}(t)$ and increase quantile noise. When the base model is simpler (HS), bias reduction from regime localization can dominate, improving both average and stress-regime calibration. Practically, this motivates TWC as a robust default, with RWC as a targeted option when regime-conditional stability is a priority.

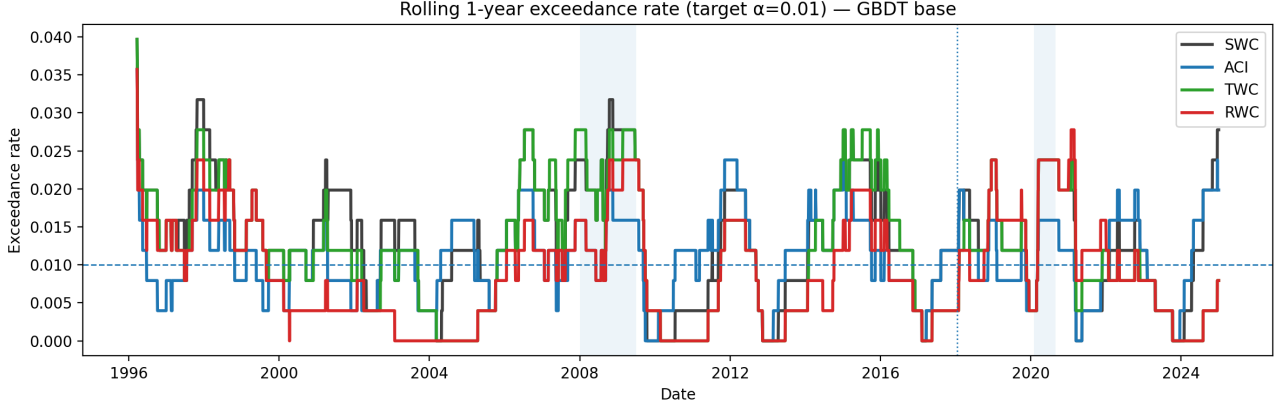


Figure 1. Rolling 1-year exceedance rate for 99% VaR ($\alpha = 0.01$) on the CRSP value-weighted index (GBDT base). The dashed horizontal line indicates the target exceedance level. The dotted vertical line marks the start of the test period. Shaded regions indicate the 2008–2009 financial crisis and the 2020 COVID shock.

Table 4. Diagnostics for weighted calibration. We report effective weighted sample size $n_{\text{eff}}(t)$ and effective memory τ_t (days) over the test period, summarizing the localization–variance tradeoff in Theorem 5.4.

Panel A: GBDT base

m	Method	med n_{eff}	p10 n_{eff}	med τ (days)	p90 τ (days)
252	SWC	252.0	252.0	126.5	126.5
252	ACI	252.0	252.0	126.5	126.5
756	TWC	382.2	382.2	182.8	182.8
756	RWC	271.1	186.1	174.4	199.5

Panel B: HS base

m	Method	med n_{eff}	p10 n_{eff}	med τ (days)	p90 τ (days)
252	SWC	252.0	252.0	126.5	126.5
252	ACI	252.0	252.0	126.5	126.5
756	TWC	199.8	199.8	100.1	100.1
756	RWC	180.8	151.4	96.0	103.6

6.5. Diagnostics and Sensitivity

Regime-stability summary. Volatility-quintile exceedances (Table 2) provide a stratified view of calibration; to summarize stability in one line per method, let \hat{e}_k be the exceedance rate (in %) in volatility quintile $k \in \{0, \dots, 4\}$ and let $e^* = 1$ be the target (in % units). Define $\Delta_k = \hat{e}_k - e^*$ (percentage points). Reg-MAE = $\frac{1}{5} \sum_k |\Delta_k|$, Reg-MaxDev = $\max_k |\Delta_k|$, and Reg-Std = $\text{Std}(\{\Delta_k\}_k)$ are reported.

Effective sample size and effective memory. To connect empirical behavior to Theorem 5.4, Table 4 summarizes $n_{\text{eff}}(t)$ and effective memory τ_t over the test period. Stronger localization (smaller h in RWC) concentrates weights on fewer past observations, lowering $n_{\text{eff}}(t)$

(more quantile noise) and altering τ_t (the effective temporal horizon). These diagnostics help identify when regime weighting is beneficial versus overly variable.

Backtesting diagnostics. As a secondary check, standard VaR backtests are applied to test-period exceedance indicators (Table 5). These tests complement average exceedance by detecting systematic miscoverage (UC) and clustering of violations (IND/CC). In nonstationary financial data, strict independence is best viewed as a diagnostic rather than a hard requirement; the primary objective is sequential exceedance control and regime-conditional stability.

Bandwidth sweep. Regime-localization strength is ablated by sweeping the kernel bandwidth h while holding (m, λ) fixed. As $h \rightarrow \infty$, the regime-similarity term becomes constant and RWC reduces to the corresponding time-weighted limit (TWC with the same m, λ). The sweep uses the same ESS safeguard: when h is small and $n_{\text{eff}}(t) < n_{\min}$, the procedure reverts to time-only weights for that step. Table 6 reports overall exceedance, average tightness, stress-regime exceedance (top volatility quintile), and n_{eff} summaries across bandwidths, making the localization–variance tradeoff explicit. To isolate the effect of h , the $h = \infty$ row corresponds to the *TWC limit under fixed (m, λ)* and may differ from separately tuned TWC results in Table 1.

7. Limitations

The guarantees rely on assumptions (weighted exchangeability or smooth drift) that are only approximations in real markets. The focus is on one-step-ahead risk for a liquid equity index; extending to multi-period horizons, illiquid assets, or portfolios with market impact introduces additional dependence and feedback effects. Finally, CRSP is propri-

Table 5. VaR backtesting diagnostics on the test period: Kupiec unconditional coverage (UC) and Christoffersen independence (IND) and conditional coverage (CC) tests applied to exceedance indicators. Note: Kupiec’s UC statistic depends only on the total number of exceedances (given N), so methods with the same exceedance count can share identical UC values even if violation timing differs.

Panel A: GBDT base										
Method	Exceedance (%)	Avg. VaR (bps)	N	Exc	LR _{uc}	p _{uc}	LR _{ind}	p _{ind}	LR _{cc}	p _{cc}
Base	5.31	146	1751	93	162.94	2.57e-37	6.36	0.012	169.31	1.72e-37
SWC	1.37	182	1751	24	2.18	0.140	4.12	0.042	6.30	0.043
ACI	1.14	200	1751	20	0.34	0.559	0.46	0.496	0.80	0.669
TWC	1.09	165	1751	19	0.12	0.724	1.64	0.201	1.76	0.414
RWC	1.14	155	1751	20	0.34	0.559	1.47	0.225	1.81	0.404

Panel B: HS base										
Method	Exceedance (%)	Avg. VaR (bps)	N	Exc	LR _{uc}	p _{uc}	LR _{ind}	p _{ind}	LR _{cc}	p _{cc}
Base	1.71	317	1751	30	7.42	0.006	2.61	0.106	10.03	0.007
SWC	1.60	358	1751	28	5.37	0.021	6.80	0.009	12.17	0.002
ACI	1.26	426	1751	22	1.08	0.300	9.57	0.002	10.65	0.005
TWC	1.48	339	1751	26	3.62	0.057	3.56	0.059	7.18	0.028
RWC	1.09	247	1751	19	0.12	0.724	5.85	0.016	5.98	0.050

Table 6. Bandwidth sweep ablation for RWC: decreasing h strengthens regime localization; as $h \rightarrow \infty$, RWC reduces to its time-weighted limit (TWC with the same m, λ).

Panel A: GBDT base						
Setting	Exceed (%)	Avg. VaR (bps)	Top-vol Exceed (%)	median n _{eff}	p10 n _{eff}	
$h = 0.5$	1.20	152	2.29	231.1	122.1	
$h = 1$	1.14	155	2.29	271.1	186.1	
$h = 2$	1.31	152	2.57	343.1	302.2	
$h = \infty$ (TWC limit)	1.09	165	2.29	382.2	382.2	

Panel B: HS base						
Setting	Exceed (%)	Avg. VaR (bps)	Top-vol Exceed (%)	median n _{eff}	p10 n _{eff}	
$h = 0.5$	1.48	212	3.71	99.0	44.6	
$h = 1$	1.09	209	3.71	142.2	80.9	
$h = 2$	1.09	247	2.86	180.8	151.4	
$h = \infty$ (TWC limit)	1.48	339	3.71	199.8	199.8	

etary; reproducible code and data-pull scripts are provided for credentialed users.

Because exact distribution-free conditional coverage is impossible in general (Barber et al., 2021), regime-conditional guarantees are necessarily approximate and depend on the informativeness of the regime embedding z_t and the effective local sample size induced by the weights.

8. Conclusion

Sequential one-sided VaR control under nonstationarity and regime structure via conformal calibration is studied. RWC is introduced, which calibrates additive safety buffers using time decay and optional regime-similarity weighting, enabling regime-aware calibration while remaining model agnostic. Empirically, TWC is a strong default under drift, and regime weighting can further improve regime-conditional stability in some settings with modest changes in conserva-

tiveness. Overall, conformal calibration provides a practical and modular reliability layer for financial risk forecasting pipelines.

Impact Statement

This work aims to improve the reliability of statistical risk controls used in financial decision-making. Better-calibrated tail risk estimates may reduce the likelihood of excessive risk-taking and improve resilience to market stress. However, risk models can also be used to scale leverage; if misused, they may contribute to systemic risk. Transparent evaluation across regimes is therefore emphasized, and code and data construction details are released to facilitate auditing and responsible deployment.

References

Adrian, T. and Shin, H. S. Procyclical leverage and value-at-risk. *The Review of Financial Studies*, 27(2):373–403, 2014. doi: 10.1093/rfs/hht068.

Angelopoulos, A. N., Candès, E. J., and Tibshirani, R. J. Conformal pid control for time series prediction. In *Advances in Neural Information Processing Systems*, volume 36, pp. 23047–23074, 2023.

Angelopoulos, A. N., Bates, S., Fisch, A., Lei, L., and Schuster, T. Conformal risk control. In *International Conference on Learning Representations*, 2024.

Barber, R. F., Candès, E. J., Ramdas, A., and Tibshirani, R. J. The limits of distribution-free conditional predictive inference. *Information and Inference: A Journal of the IMA*, 2021. doi: 10.1093/imaiai/iaaa017.

Barber, R. F., Candès, E. J., Ramdas, A., and Tibshirani, R. J. Conformal prediction beyond exchangeability. *The Annals of Statistics*, 51(2):816–845, 2023. doi: 10.1214/23-AOS2276.

Basak, S. and Shapiro, A. Value-at-risk-based risk management: Optimal policies and asset prices. *The Review of Financial Studies*, 14(2):371–405, 2001. doi: 10.1093/rfs/14.2.371.

Berkowitz, J. and O’Brien, J. How accurate are value-at-risk models at commercial banks? *The Journal of Finance*, 57(3):1093–1111, 2002. doi: 10.1111/1540-6261.00455.

Christoffersen, P. F. Evaluating interval forecasts. *International Economic Review*, 39(4):841–862, 1998.

Ding, L., Hébert-Johnson, U., Wang, R., and Tibshirani, R. J. Class-conditional conformal prediction with many classes. In *Advances in Neural Information Processing Systems*, 2023.

Engle, R. F. and Manganelli, S. Caviar: Conditional autoregressive value at risk by regression quantiles. *Journal of Business & Economic Statistics*, 22(4):367–381, 2004.

Engle, R. F. and Rangel, J. G. The spline-garch model for low-frequency volatility and its global macroeconomic causes. *The Review of Financial Studies*, 21(3):1187–1222, 2008.

Gibbs, I. and Candès, E. J. Adaptive conformal inference under distribution shift. In *Advances in Neural Information Processing Systems*, volume 34, pp. 1660–1672, 2021.

Gibbs, I. and Candès, E. J. Conformal inference for online prediction with arbitrary distribution shifts. *Journal of Machine Learning Research*, 25(86):1–36, 2024.

Gray, S. F. Modeling the conditional distribution of interest rates as a regime-switching process. *Journal of Financial Economics*, 42(1):27–62, 1996.

Guan, L. Conformal prediction with localization. *Biometrika*, 110(1), 2023.

Hamilton, J. D. A new approach to the economic analysis of nonstationary time series and the business cycle. *Econometrica*, 57(2):357–384, 1989.

Kupiec, P. H. Techniques for verifying the accuracy of risk measurement models. *Journal of Derivatives*, 3(2):73–84, 1995.

Rockafellar, R. T. and Uryasev, S. Optimization of conditional value-at-risk. *Journal of Risk*, 2(3):21–41, 2000.

Romano, Y., Patterson, E., and Candès, E. J. Conformalized quantile regression. In *Advances in Neural Information Processing Systems*, volume 32, pp. 3538–3548, 2019.

Shafer, G. and Vovk, V. A tutorial on conformal prediction. *Journal of Machine Learning Research*, 9:371–421, 2008.

Snell, J. C. and Griffiths, T. L. Conformal prediction as Bayesian quadrature. In Singh, A., Fazel, M., Hsu, D., Lacoste-Julien, S., Berkenkamp, F., Maharaj, T., Wagstaff, K., and Zhu, J. (eds.), *Proceedings of the 42nd International Conference on Machine Learning*, volume 267 of *Proceedings of Machine Learning Research*, pp. 56068–56084. PMLR, 13–19 Jul 2025.

Tibshirani, R. J., Foygel Barber, R., Candès, E. J., and Ramdas, A. Conformal prediction under covariate shift. *Advances in Neural Information Processing Systems*, 32, 2019.

Vovk, V., Gammerman, A., and Shafer, G. *Algorithmic Learning in a Random World*. Springer, New York, 2005.

Xu, C. and Xie, Y. Conformal prediction interval for dynamic time-series. In *Proceedings of the 38th International Conference on Machine Learning*, volume 139 of *Proceedings of Machine Learning Research*, pp. 11559–11569. PMLR, 2021.

Xu, C. and Xie, Y. Sequential predictive conformal inference for time series. In *Proceedings of the 40th International Conference on Machine Learning*, volume 202 of *Proceedings of Machine Learning Research*, pp. 38707–38727. PMLR, 2023.

A. Implementation details

Weighted quantile and finite-sample correction. Given values v_1, \dots, v_n and nonnegative weights \tilde{w}_i summing to one, the weighted γ -quantile is

$$Q_{\gamma}^{\tilde{w}}(\{v_i\}) := \inf \left\{ q \in \mathbb{R} : \sum_{i=1}^n \tilde{w}_i \mathbf{1}\{v_i \leq q\} \geq \gamma \right\}.$$

We implement this via sorting v_i and accumulating the sorted weights until the cumulative mass exceeds γ .

At time t , let $w_i(t) \geq 0$ be the unnormalized calibration weights for $i \in \mathcal{I}_t$ (as in (3)), and define $W_t := \sum_{i \in \mathcal{I}_t} w_i(t)$ and normalized weights $\tilde{w}_i(t) := w_i(t)/W_t$. Let $w_t(t)$ denote the weight assigned to the current test point (for (3), $w_t(t) = 1$). For exact finite-sample weighted conformal coverage (Theorem 5.2) one can use the inflated level

$$\rho_t := \min \left\{ 1, (1 - \alpha) \left(1 + \frac{w_t(t)}{W_t} \right) \right\},$$

and set $\hat{c}_t := Q_{\rho_t}^{\tilde{w}(t)}(\{s_i\}_{i \in \mathcal{I}_t})$ and $U_t := \hat{q}_t + \hat{c}_t$. In the experiments we use $\rho_t = 1 - \alpha$ for simplicity; when W_t (or $n_{\text{eff}}(t)$) is large the practical difference is negligible.

Effective weighted sample size and effective memory. We define the effective weighted sample size

$$n_{\text{eff}}(t) := \frac{1}{\sum_{i \in \mathcal{I}_t} \tilde{w}_i(t)^2},$$

and the effective lag (effective memory) under the normalized weights

$$\tau_t := \sum_{i \in \mathcal{I}_t} \tilde{w}_i(t) (t - i).$$

ESS safeguard (implementation). Regime localization can concentrate weights on a small subset of past observations, reducing the effective calibration sample size $n_{\text{eff}}(t) = 1 / \sum_{i \in \mathcal{I}_t} \tilde{w}_i(t)^2$ and increasing quantile-estimation variance (cf. Theorem 5.4). To prevent unstable calibration when locally relevant history is limited, we apply an ESS safeguard: if $n_{\text{eff}}(t) < n_{\min}$ we drop the regime kernel for that step (set $K_h \equiv 1$) and compute the calibration quantile using time-only weights (i.e., the TWC weights) for that step. In our experiments we use $n_{\min} = 100$ for the GBDT base and $n_{\min} = 30$ for the HS base.

Regime embedding used in experiments. In all experiments we use a two-dimensional regime embedding $z_t = (\text{RV21}_t, \text{MAR5}_t)$ computed from lagged portfolio returns:

$$\text{RV21}_t := \sqrt{252} \text{Std}(r_{t-21:t-1}^{\text{port}}), \text{MAR5}_t := \frac{1}{5} \sum_{j=1}^5 |r_{t-j}^{\text{port}}|.$$

Both features use only information available up through time $t-1$ (consistent with the timing convention in Section 3). Before computing K_h , each coordinate of z_t is standardized to zero mean and unit variance using pre-test statistics.

ACI baseline details. We implement ACI following [Gibbs & Candès \(2021\)](#) using a sliding calibration window of size $m = 252$ and an adaptive miscoverage level α_t . Initialize $\alpha_{t_0} = \alpha$ and update

$$\alpha_{t+1} = \Pi_{[\alpha_{\min}, \alpha_{\max}]}(\alpha_t + \gamma(\alpha - \mathbf{1}\{y_t > U_t\})),$$

where Π clips to $[\alpha_{\min}, \alpha_{\max}]$ (we use $\alpha_{\min} = 10^{-4}$ and $\alpha_{\max} = 0.2$) and γ is tuned on validation using the same criterion as above. At time t , ACI computes \hat{c}_t as the empirical $(1 - \alpha_t)$ -quantile of the last m conformity scores.

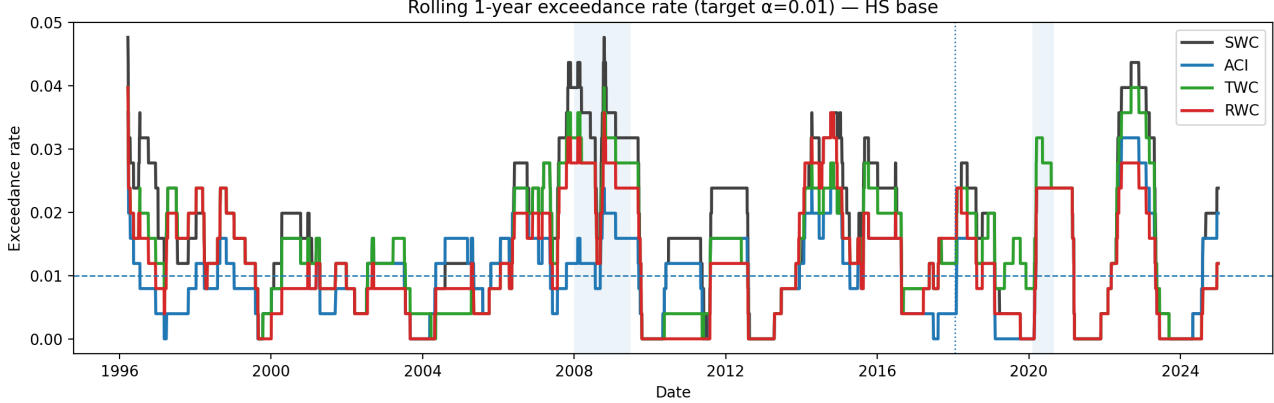


Figure 2. Rolling 1-year exceedance rate for 99% VaR ($\alpha = 0.01$) on the CRSP value-weighted index (HS base). The dashed horizontal line indicates the target exceedance level. The dotted vertical line marks the start of the test period. Shaded regions indicate the 2008–2009 financial crisis and the 2020 COVID shock.

Table 7. Hyperparameters used in the main experiments (selected on the validation period). For TWC, $h = \infty$ denotes no regime weighting ($K_h \equiv 1$). For SWC/ACI, λ and h are not used (uniform weights within the sliding window). For RWC we additionally use an effective-sample-size safeguard: if $n_{\text{eff}}(t) < n_{\text{eff,min}}$, we fall back to TWC weights for that time t .

Base	Method	m	λ	h	γ (ACI)	$n_{\text{eff,min}}$
GBDT	SWC	252	—	—	—	—
GBDT	TWC	756	0.005	∞	—	—
GBDT	RWC	756	0.005	1.0	—	100
GBDT	ACI	252	—	—	0.005	—
HS	SWC	252	—	—	—	—
HS	TWC	756	0.010	∞	—	—
HS	RWC	756	0.010	2.0	—	30
HS	ACI	252	—	—	0.002	—

B. Proofs

Proof sketch for Theorem 5.2. Fix time t and condition on (x_t, z_t) . Under weighted exchangeability (Assumption 5.1), the joint distribution of the weighted multiset $\{(s_i, w_i(t))\}_{i \in \mathcal{I}_t} \cup \{(s_t, w_t(t))\}$ is invariant to permutations. Following Tibshirani et al. (2019), define the (randomized) weighted conformal p -value for the one-sided score as

$$p_t := \frac{\sum_{i \in \mathcal{I}_t} w_i(t) \mathbf{1}\{s_i \geq s_t\} + w_t(t) U}{W_t + w_t(t)},$$

where $U \sim \text{Unif}(0, 1)$ is independent and breaks ties. Weighted exchangeability implies p_t is super-uniform, i.e., $\mathbb{P}(p_t \leq \alpha \mid x_t, z_t) \leq \alpha$. Equivalently, with probability at least $1 - \alpha$, the test score s_t is not in the upper α -tail of the weighted empirical distribution. The choice of ρ_t in (5) (implemented in Appendix A) corresponds exactly to the acceptance region $\{p_t > \alpha\}$, which yields $\mathbb{P}(s_t \leq \hat{c}_t \mid x_t, z_t) \geq 1 - \alpha$. Since $s_t = y_t - \hat{q}_t$, the event $s_t \leq \hat{c}_t$ is equivalent to $y_t \leq \hat{q}_t + \hat{c}_t = U_t$, proving the claim.

Proof sketch for Theorem 5.4. Let

$$\hat{F}_t^w(u) := \sum_{i \in \mathcal{I}_t} \tilde{w}_i(t) \mathbf{1}\{s_i \leq u\}$$

be the weighted empirical CDF of scores, and compare it to the target conditional score CDF $F_t(u \mid z_t)$.

(*Bias due to regime mismatch and time drift.*) Add and subtract $F_i(u \mid z_t)$ and apply the triangle inequality:

$$\begin{aligned} \left| \mathbb{E}[\hat{F}_t^w(u)] - F_t(u \mid z_t) \right| &\leq \sum_{i \in \mathcal{I}_t} \tilde{w}_i(t) \left| F_i(u \mid z_i) - F_i(u \mid z_t) \right| \\ &\quad + \sum_{i \in \mathcal{I}_t} \tilde{w}_i(t) \left| F_i(u \mid z_t) - F_t(u \mid z_t) \right|. \end{aligned}$$

By Assumption 5.3, the first term is bounded by $L_z \sum_{i \in \mathcal{I}_t} \tilde{w}_i(t) \|z_i - z_t\| = O(L_z h)$ (kernel concentration), and the second term is bounded by $L_t \sum_{i \in \mathcal{I}_t} \tilde{w}_i(t)(t - i) = L_t \tau_t$ (by definition). Thus the bias is of order $O(L_z h) + O(L_t \tau_t)$.

(*Stochastic term controlled by effective sample size.*) For each fixed u , $\hat{F}_t^w(u)$ is a weighted average of bounded random variables. Under conditional independence (or sufficiently weak dependence, e.g. standard mixing), concentration for weighted sums yields

$$\left| \hat{F}_t^w(u) - \mathbb{E}[\hat{F}_t^w(u)] \right| = O\left(\sqrt{\sum_{i \in \mathcal{I}_t} \tilde{w}_i(t)^2} \right) = O\left(\sqrt{\frac{1}{n_{\text{eff}}(t)}} \right),$$

up to log factors for uniform-in- u control.

(*CDF error \Rightarrow quantile error \Rightarrow coverage gap.*) Under mild regularity (e.g., local continuity / positive slope of $F_t(\cdot \mid z_t)$ near the target quantile), a bound on $\sup_u |\hat{F}_t^w(u) - F_t(u \mid z_t)|$ implies a corresponding bound on the weighted-quantile error for \hat{c}_t and hence on $\mathbb{P}(s_t \leq \hat{c}_t \mid z_t)$. Translating back via $s_t = y_t - \hat{q}_t$ yields the stated coverage bound with $\varepsilon_t = O(L_z h) + O(L_t \tau_t) + O(\sqrt{1/n_{\text{eff}}(t)})$.

Remark (finite-sample correction). Weighted conformal validity statements typically use a small finite-sample correction to the quantile level that depends on the total calibration weight W_t (and the test-point weight), analogous to the $(m+1)$ correction in standard conformal prediction (Tibshirani et al., 2019). In our experiments we use the simpler level $1 - \alpha$; when W_t (or $n_{\text{eff}}(t)$) is large, the difference is negligible.